RERTR 2014 – 35TH INTERNATIONAL MEETING ON
REDUCED ENRICHMENT FOR RESEARCH AND TEST REACTORS

OCTOBER 12-16, 2014
IAEA VIENNA INTERNATIONAL CENTER
VIENNA, AUSTRIA

Bonding Toughness Measurements in LEU Fuel Plates

C. Liu[1], N.A. Mara[2], M.L. Lovato[1], D.J. Alexander[1], K.D. Clarke[1], K.J. Hollis[1], D.E. Dombrowski[1]
[1] Materials Science and Technology Division
[2] Materials Physics and Applications Division
Los Alamos National Laboratory, Los Alamos, NM 87545, USA

W.M. Mook
Center for Integrated Nanotechnologies
Sandia National Laboratories, Albuquerque, NM 87123, USA

ABSTRACT

Recent research into U-10%Mo/Zr/Al plate fuel assemblies has illustrated the importance of fundamentally understanding interfacial mechanical behavior both before and after exposure to irradiation environments. The parameters and phenomena that have been noted include existence of stress gradients at interfaces and their influence on bond strength, and strength and fracture behavior of the various interfaces before and after irradiation. Bending and tension tests have been used to gain some insight on the mechanical behavior of the composite plate, but neither method can isolate the mechanical behavior of a specific bond. Here we present the fracture behavior of Al/Zr and Zr/U-10%Mo bonds as measured by two newly developed methods: (1) Miniature hydraulic bulge test and (2) MiniCantilever beam bending. Using both methods, a crack was successfully initiated along the interface, providing for quantitative measurement of upper bound and lower bound values for the fracture energy release rate associated with fracture in the vicinity of the specific interfaces. Detailed discussions of the schemes of preparing and conducting both testing types, and computing various quantities required for the determination of the energy release rate are presented.

1. Introduction

This work supports the National Nuclear Security Agency's (NNSA) Global Threat Reduction Initiative (GTRI) Conversion program. The purpose of the Department of Energy's National Nuclear Security Administration's Office of Global Threat Reduction's Conversion program, formerly known as the Reduced Enrichment for Research and Test Reactors (RERTR) program,

is to work with research reactors operators worldwide in an effort to convert reactors from the use of highly enriched uranium (HEU) fuel to the use of low enriched uranium (LEU). The monolithic fuel foils are to be co-rolled with Zr and clad with 6061-Al using hot isostatic pressing (HIP). The resulting fuel plate contains Al/Al, Al/Zr, and Zr/U-10%Mo bonds whose integrity is critical to performance, including during subsequent processing, shipping, and in-reactor service.

Two experimental techniques were developed to measure the interfacial toughness of the LEU fuel plates. One is the miniature bulge test and the other is the SEM *in situ* mini-cantilever bending technique. Results of the experimental measurement of the fracture behavior of Al/Zr and Al/Zr/DU-10%Mo interfaces is presented in this article.

2. Miniature bulge test for measuring interfacial toughness of Al/Zr/DU-10%Mo

A technique of combining the miniature bulge test and the optical three-dimensional digital image correlation (3D-DIC) was applied to measure the interfacial fracture toughness of the LEU fuel plate.

The miniature bulge test setup is shown schematically in Figure 1, where two CCD (charge-coupled device) cameras are arranged in front of the testing sample. The entire surface of the bulge has to be "seen" by both cameras in order to measure the shape of the bulge. At each instant of time during the deformation, the 3D profile of the sample surface is quantified. Repeating the process at every instant of time during the test, the evolution of the bulge profile can be obtained, and consequently, evolution of the displacement field on the sample surface can be determined. From the geometric profile of the evolving bulge, the strain field and the curvature field over the bulge surface can be calculated. Such information is necessary for evaluating the mechanical properties of the interface. The details of the test system are described and discussed in [1].

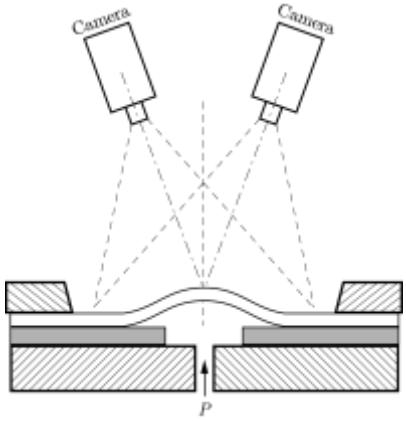

Figure 1: Schematic sketch of the miniature bulge test setup.

One of the interfaces in the monolithic LEU fuel plate is between zirconium and aluminum cladding. In the monolithic LEU fuel design, a thin coating of zirconium is either co-rolled or plasma-sprayed onto the DU-10%Mo foil to form a diffusion barrier. In order to isolate the zirconium/aluminum interface and determine its bonding strength and toughness, plates with zirconium thin foil (with nominal thickness of 0.254 mm) sandwiched with aluminum cladding were manufactured following the same HIPing procedure for making LEU plates described in previous sections. Bulge test specimens were then machined from these plates. In this section, we discuss and present the experimental results regarding the aluminum/zirconium interface.

In these series of bulge tests, two different kinds of bulge test specimens are considered and they are shown in Figure 2. In the first kind of specimens, the recess is only through the thickness of the aluminum cladding on one side of the zirconium. The aluminum cladding on the other side of the zirconium foil is machined away, so that in the bulge test, the zirconium foil will be deformed as shown in Figure 2(a). In the second kind of specimens, the circular recess is machined through both the aluminum cladding and the zirconium foil and the aluminum

cladding on the other side of the zirconium foil is intact. Therefore, in the bulge test, the aluminum cladding is deformed, as shown in Figure 2(b).

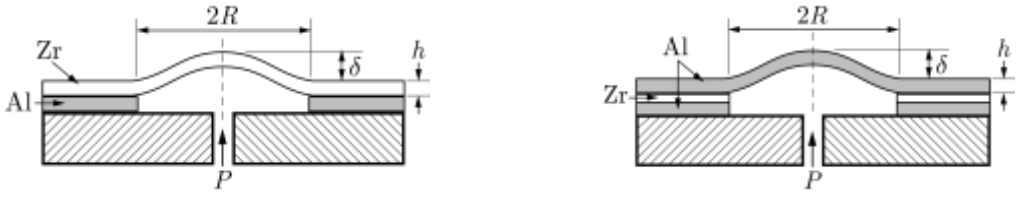

(a) (b)

Figure 2: Specimen assemblies for measuring aluminum/zirconium interface: (a) By deforming zirconium foil. (b) By deforming aluminum foil.

Figure 3(a) presents the overall response of the Zr/Al bulge specimen AZ08, where the applied pressure P is plotted as a function of the maximum deflection of the bulge δ normalized by the initial zirconium foil thickness h. Note that the applied pressure P monotonically increases first, as the bulge continues to deform, then pressure P reaches a maximum at moment F, after which it gradually decreases. The profiles of the evolving bulge obtained by using 3D-DIC are shown in Figure 3(b), at the moments of time indicated in Figure 3(a).

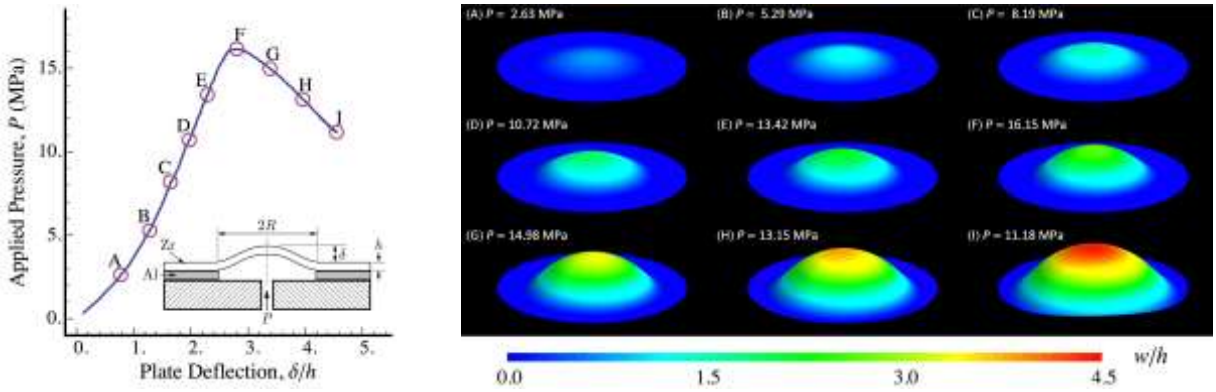

(a) (b)

Figure 3: (a) Overall response of the Zr/Al bulge specimen AZ08. (b) Evolution of the bulge profile of specimen AZ08 at selected moments of time during the test.

From an energetic point of view, during the process of bulge formation and extension, the total energy input from the external loading is partitioned into two parts: (1) the strain energy of the deforming bulge, where the deformation can be either elastic or elastoplastic, and (2) the surface energy for generating debonded new surfaces along the interface between the thin foil and the substrate. The total energy E can be determined by the integration of applied pressure P over the bulge volume V, which can be computed from the bulge profile shown in Figure 3(b). The strain energy of the deforming bulge W can be calculated from the strain and curvature measurement over the bulge surface and the constitutive relation of the Zr foil, which ahs been determined by separate experiment. The variations of E and W for specimen AZ08 are shown in Figure 4(a). The difference $\Pi = E - W$ thus represents the delamination energy that is used to generate new surface along the Zr/Al interface.

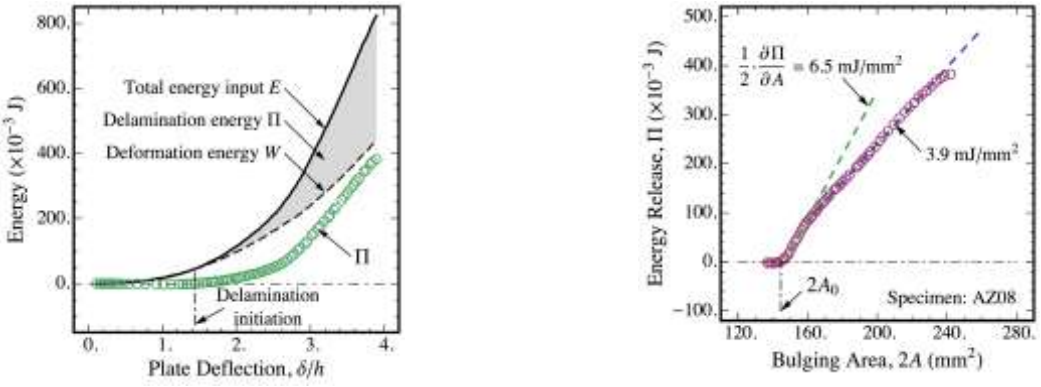

(a) (b)

Figure 4: (a) Energy partition of specimen AZ08. (b) Variation of energy release Π, or delamination energy, as function of bulging area A for specimen AZ08.

The energy release, or delamination energy Π, of specimen AZ08 is plotted against the bulging area A in Figure 4(b). The slope, $(\partial\Pi/\partial A)/2$, is the energy release rate γ, or the fracture toughness, of the Zr/Al interface. For delamination initiation we found that $\gamma = 6.5\ \mathrm{mJ/mm^2}$, and this toughness quickly reduces to 3.9 mJ/mm^2. Meanwhile, bulge specimens with the configuration as shown in Figure 2(b), where the Al cladding is deformed, are also tested and we found that the energy release rate γ ranges from 4.1 to 6.4 mJ/mm^2.

Miniature bulge test of samples containing Al/Zr/DU-10%Mo interfaces are studied as well. The plate was manufactured at LANL and contains DU-10%Mo with co-rolled Zr coating sandwiched between Al cladding, and went through the HIPing cycle. Figure 5(a) shows the overall response of the bulge test of specimen OSU-2R2, where the Al cladding is deformed. The bulge profiles of OSU-2R2 are presented in Figure 5(b). At moment D, the applied hydraulic pressure P has a slight drop and the deflection of the Al foil δ has a slight jump, indicated by the arrow in the plot. This sudden jump is associated with the local, unstable delamination along the interface. At moment E, the unstable delamination was arrested and as the pressure continues to rise, interfacial delamination proceeds further. At moment F, where the applied pressure reaches maximum, the bulge sample failed by the Al foil burst along the edge of the bulge.

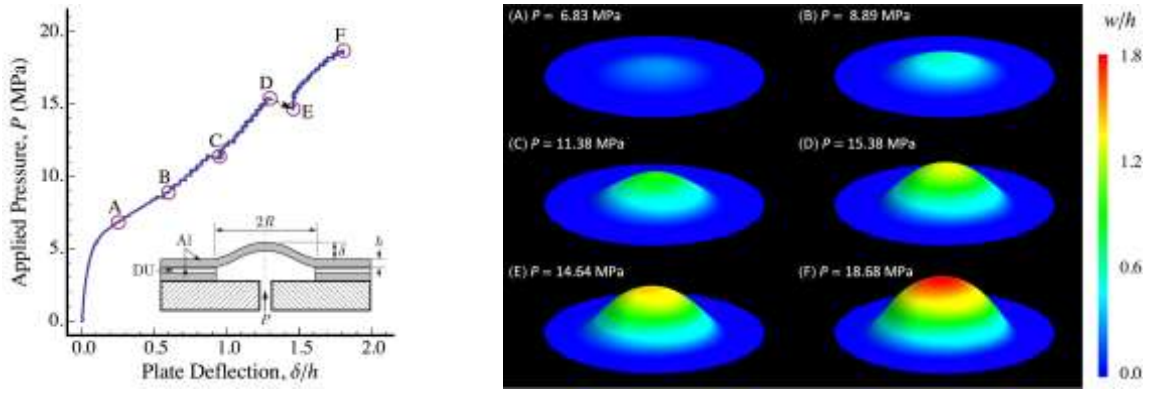

(a) (b)

Figure 5: (a) Overall response of specimen OSU-2R2, where aluminum foil is deformed. (b) Evolution of the bulge profile of specimen OSU-2R2 at selected moments.

The total energy input E and the deformation energy of the bulge W are computed, based on the 3D-DIC measurement, and they are plotted against the deflection of the bulge δ/h in Figure 6(a) for specimen OSU-2R2, where the dashed line is the deformation energy and the solid line the total energy input. Initially E and W are equal and as the deformation continues, the total energy input E and the deformation energy W deviate from each other. The energy release, or the delamination energy $\Pi = E - W$, is also shown in Figure 6(a) as open symbols. The energy release Π is plotted against the bulging area A in Figure 6(b). Note that the sudden jump during the loading indicated in Figure 5(a), is also shown in Figure 6 as dashed arrows. We see from Figure 6(b) that prior to and after the sudden jump, the relation between the energy release Π and the total bulging area $2A$ can be approximated as linear, and their slopes, $(\partial\Pi/\partial A)/2$, represent the energy release rate, or the fracture toughness. These fracture toughness can be estimated to be 2.4 mJ/mm^2 and 3.5 mJ/mm^2, respectively, from Figure 6(b).

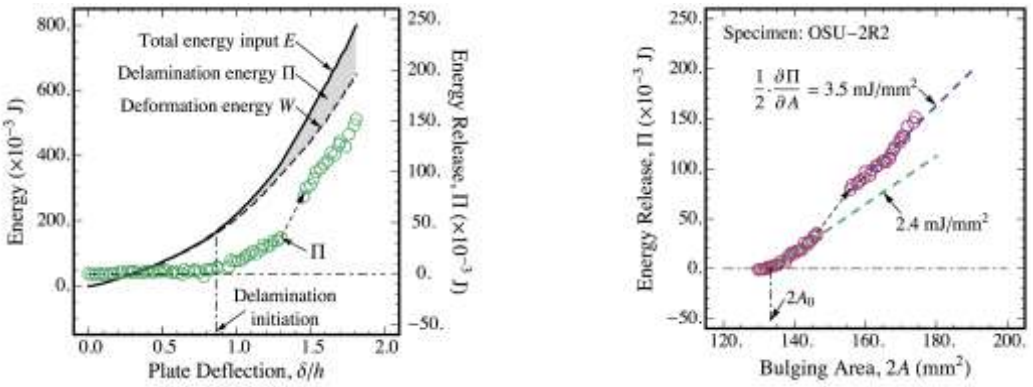

(a) (b)

Figure 6: (a) Energy partition of specimen OSU-2R2; (b) Variation of energy release Π, or delamination energy, as function of bulging area A for specimen OSU-2R2.

Total of 7 specimens containing Al/Zr/DU-10%Mo interfaces, shown as the insert in Figure 5(a), were tested. When we focus on the initial initiation of the delamination, we find that the interfacial fracture toughness measurement is quite consistent and we estimate the average value of the fracture toughness to be $\gamma = (\partial\Pi/\partial A)/2 = 2.51 \pm 0.67$ mJ/mm^2. Note that this value is lower than what we have measured from both the Al/Al interface and the Al/Zr interface [1].

3. SEM *in situ* mini-cantilever beam bending of U-10%Mo/Zr/Al fuel elements

The fracture behavior of Al/Zr and Zr/DU-10%Mo interfaces was measured via the minicantilever bend technique [2]. The goal of this work is to develop an experimental method to quantify the adhesion energy (i.e., the toughness) of individual interfaces within a fuel plate assembly. The method should also be executable within a hot cell. The main experimental challenge arises from the geometry of the fuel plate assembly since the interfaces of interest are composed from materials that are sub-mm in thickness. Therefore micromechanical testing inside of a microscope (in this case, a scanning electron microscope) is ideal.

In order to drive fracture at this length scale along a specific interface, a notched-cantilever beam geometry is used as seen in the schematic in Figure 7. The cantilever beam is bent using a microindenter that tracks both load and displacement while taking images with the microscope. The notch acts as a stress concentrator and a sharp crack should nucleate from it along the interface of interest. The dimensions of the cantilever beams are limited in length by the individual layer thicknesses of the fuel assembly and in cross-sectional area by the maximum load that the indentation load cell can generate (for the CINT SEM-indenter the maximum load is approximately 1N). Al-Al HIP bonded beams were machined to dimensions of 0.75 mm long with a cross-section of 0.25× 0.25 mm. The Al/Zr and Zr/ DU-10%Mo beams were machined to 0.25 mm long with a nominal cross-section of 0.10×0.10 mm. The minicantilever beams were machined with a MiniMill 4 from MiniTech Industries. This equipment has a positioning accuracy of 2.5 μm that allows the machinist to position an interface at the base of the beam.

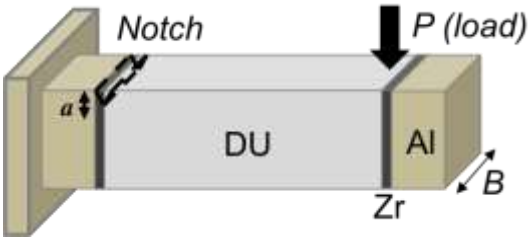

Figure 7: Beam schematic: the Al and DU are 250 μm wide, and the Zr is 30 μm wide. *B* is the width of of the beam and *a* represents the notch length, then during testing, the length of notch plus crack. Load (*P*) is applied by the microindenter for driving the crack growth along the prescribed interface.

Notches were fabricated by one of two methods; femtosecond laser ablation, or milling with a focused ion beam (FIB). The femtosecond laser ablation is fast, taking approximately 1 minute to notch a single beam, although it has lower resolution and spatial accuracy. FIB-milling is relatively slow (it can take 8 hours to notch a single beam) but it is very accurate (spatial accuracy < 100 nm).

The cantilever beams were tested inside of one of two SEM's. The FEI Quanta at the Center for Integrated Nanotechnologies (CINT), an international Department of Energy (DOE) user facility at Los Alamos National Laboratory (LANL) was used for non-DU containing materials, while the FEI Helios at the Electron Microscopy Lab (EML) in the Materials Science Laboratory (MSL) at LANL was used for materials that contained DU. The in-house built CINT SEM-Indenter was used to test cantilever beams that could be plastically deformed at loads under 1 N is seen in Figure 8. During testing, the beams were positioned 90° to the SEM electron beam such that the side of the beam and any fracture along the interface in question could be imaged throughout the entire load-unload process. In this way it was possible to monitor interfacial crack length as a function of load in real time. The displacement rate during all of the tests was less than 1 μm/sec. The load frame is inherently displacement-controlled, however the displacement rate changes due to compliance of the load cell, i.e., displacement rates during the elastic loading is relatively low while rates during the plastic portion of the bending experiment approach 1 μm/sec. Movies of the experiments were created by compiling one image per second from the SEM and syncing to the load-displacement

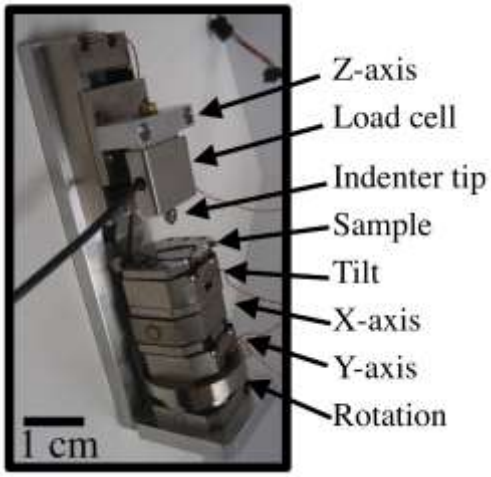

Figure 8: Schematic of custom-built CINT Micromechanical Tester with 1 N load cell used for in-situ straining in the SEM.

data from the load frame.

For cantilever beams that required higher loads, the Nanoindenter-XP was used (maximum load of 10 N) and conducted at a displacement rate of 50 nm/sec. For this test, the bending was intermittently paused and beams were imaged in the SEM when crack growth was evident on the load-displacement curve. The test was then resumed in the nanoindenter.

To assure that fracture propagated along the Al/Zr interface, the samples were notched with a femtosecond laser. The notches made by the laser varied in depth and proximity to the Al/Zr interface, but were in general within 3 μm of the interface and had a depth of approximately 10 μm. Figure 9 shows two deformed Al/Zr cantilevers with notched Al-Zr interfaces. In all tests conducted, fracture occurred at the Al/Zr interface. Interestingly, the position of the notch did not seem to affect the path of the crack, as failure always occurred at the Al/Zr interface, even if the notch was located a few microns from the interface itself. This behavior is evident in the cantilever seen in the foreground of Figure 9, where the notch was located in the Zr, but fracture still proceeded at the Al-Zr interface.

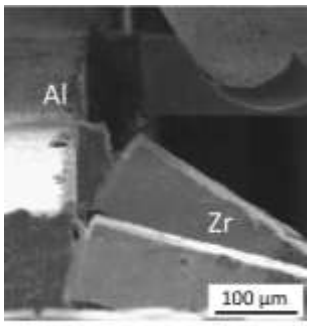

Figure 9: Al/Zr notched beams after bend testing.

Figure 10(a) shows the load-displacement response of the Al/Zr notched beam in addition to images taken from the movie that were used to calculate crack growth. From this data, fracture energy dissipation rates can be calculated [3]. The fracture energy dissipation rate (D) is $D = dE/dA = (dU/da)/2B$, where dE is the total energy dissipated, i.e., it is the area under the load-displacement curve. The new surface area of the crack is dA which is the width of the beam, B, multiplied by twice the new crack length, $2a$, accounting for the two faces of the crack. The fracture energy dissipation rate for the Al/Zr interface is estimated ranging from 3.7−5 mJ/mm^2. This is in close agreement with values obtained via bulge testing mentioned earlier in this article.

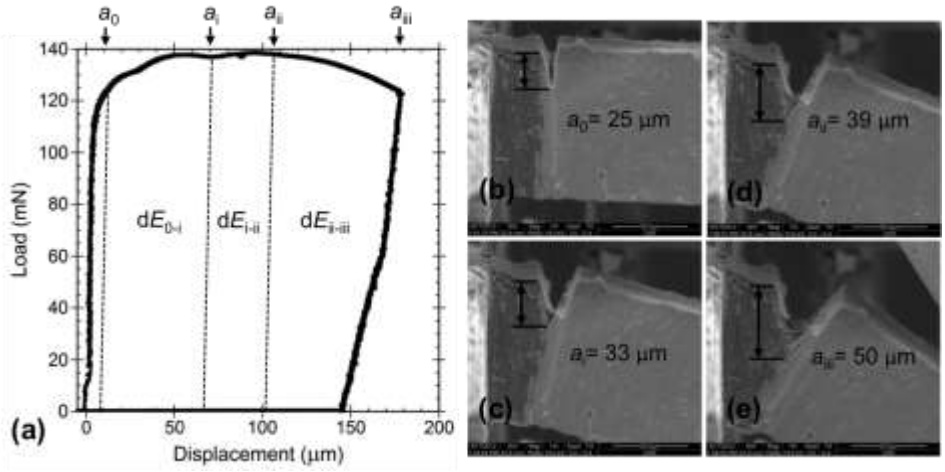

Figure 10: Al/Zr beam deflection showing (a) partitioning of energy, i.e., area under the load-displacement curve along with (b-e) four frames taken from the SEM in-situ movie with estimated

During the portions of the load-displacement curve where crack growth occurs (a = 25 to 50

μm), the energy dissipation rate only varies minimally, suggesting that despite the varying amounts of plastic deformation in the Al phase as the test progresses, the energy dissipation rate for the system remains the same. This further suggests that the amount of energy dissipated via plastic deformation of Al is very close to that required for crack propagation along the Al/Zr interface. An EPFM analysis should become increasingly applicable in future work when materials and interfaces embrittled by the effects of radiation.

For the DU-containing materials, two sets of beams were tested. One set had the Zr/DU-10%Mo and Al/Zr interface buried within the substrate while the other had the both of the interface contained within the cantilever beam itself. In both cases, the beams were notched via FIB milling. For the buried interfaces, the FIB was also used to cut away excess material and expose only the Zr/DU-10%Mo interface. As will be shown, interface location with respect to the base of the beam is very important. Fracture only occurs along and near the Zr/DU-10%Mo interface when the interfaces are buried (then notched and excavated via FIB) beneath the base of the beam. When the interfaces are contained within the beam, fracture occurs along the Al/Zr interface even though the Zr/DU-10%Mo interface is notched. In this case Al plastically deforms at a stress level that is inadequate to drive fracture along the Zr/DU-10%Mo interface. A comparison showing the importance of interface location can be seen in Figure 11.

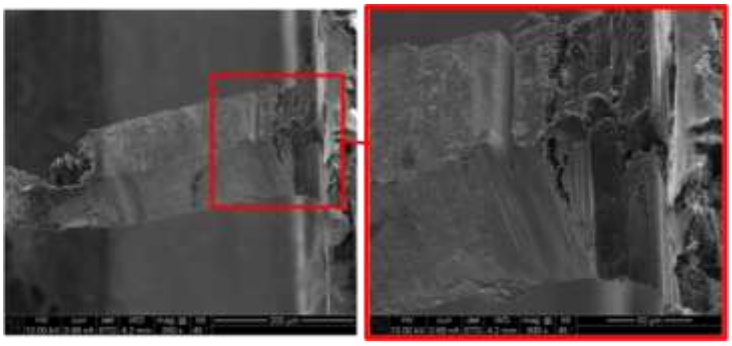

Figure 11: The notch for this beam was located at the Zr/DU-10%Mo interface, however the crack propagated along the Al/Zr interface. This behavior was not seen for cantilever beams with both interfaces located under the base of the beam.

The DU beams with the buried Zr/DU-10%Mo interface had a tapered geometry due to non-optimized milling. The larger cross-sectional area at the base required higher loads in order to

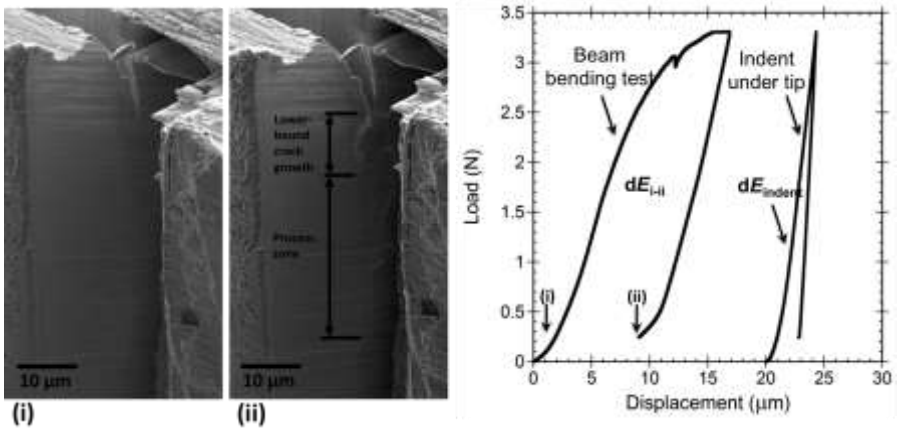

Figure 12: Fracture along the Zr/DU-10%Mo interface where image (i) is the initial notch before the test, the location of which is shown on the load-displacement curve, and image (ii) is after the first compression as shown on the load-displacement curve. Since the maximum load here was greater than 3 N, plastic deformation was generated beneath the tip and is represented by area under the curve. In order to account for this deformation, the area generated from the indent is subtracted from the overall energy of the test.

plastically deform them enough to drive fracture. Therefore the hybrid testing technique (loading the cantilever beam using the Nanoindenter XP, pause after crack growth to image in the SEM) was used. As can be seen by comparing image (i) to image (ii) in Figure 12, the notch has initiated a crack that extends towards and along the Zr/DU-10%Mo interface by approximately 12.9 μm. Since the base of the beam is 185 μm wide, the new area generated is approximately 4790 μm^2. In front of the crack-tip, there is an extended area of slip traces that could be considered a process zone. A lower bound estimate for new surface area is 4790 μm^2. The energy expended during the bending is the area under the load-displacement curve and is 2.30×10^7 mN×nm. A portion of this energy was due to plastic deformation under the indenter tip that is represented by the load-displacement response of an indent into DU-10%Mo in Figure 12 that is offset along the displacement axis by 20 μm. The area corresponding to the indent is 0.23×10^7 mN×nm giving the total energy expended at the base of the beam as 2.07×10^7 mN×nm. Therefore the strain energy dissipation rate is $D = 4.3\ \mathrm{mJ/mm^2}$.

Another example of Zr/DU-10%Mo interfacial fracture is shown in Figure 13. In order to initiate a sharp crack from the notch, extra energy was necessary as is seen when calculating the energy from Figure 13, image (i) to image (ii). Once the sharp crack was initiated, energies decreased to 5.9 mJ/mm^2. On average the energy dissipation rate of the Zr/DU-10%Mo interface was 4−6 mJ/mm^2.

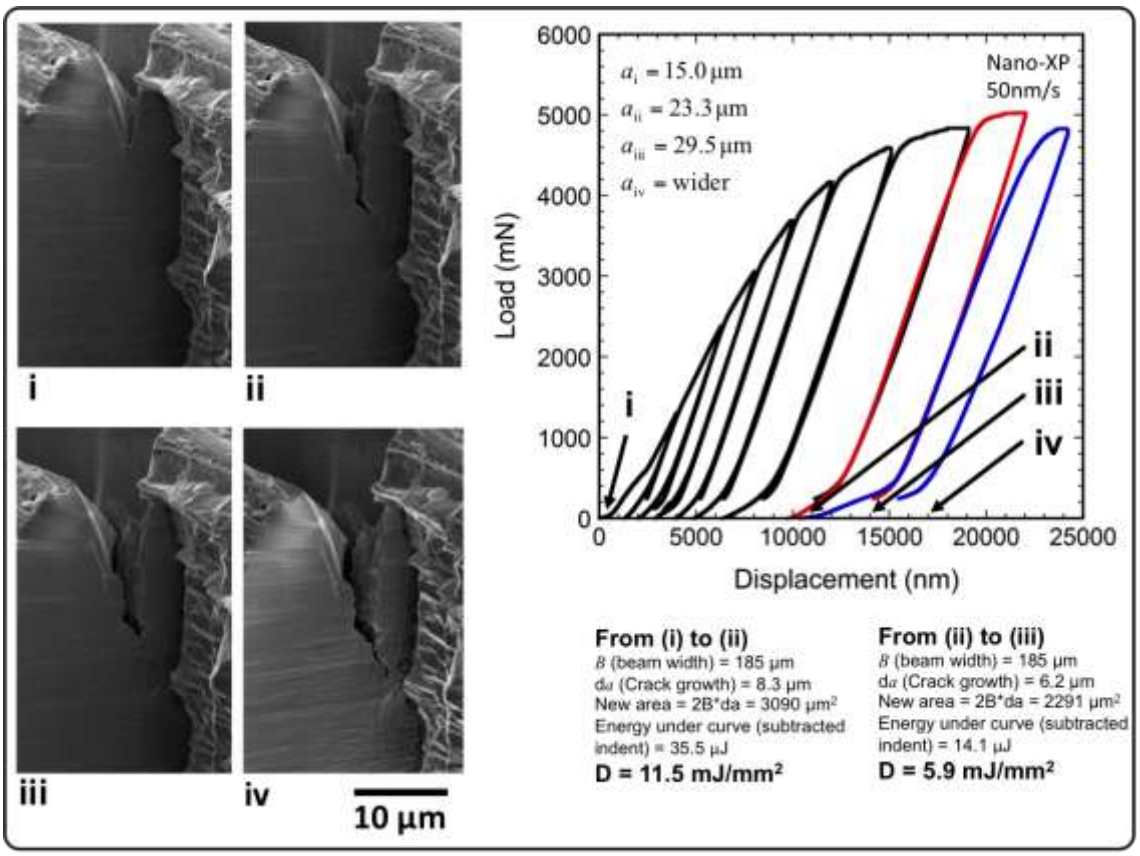

Figure 13: Zr/DU-10%Mo interfacial fracture where strain energy dissipation rates were initially high. Once a sharp crack was nucleated as seen in image (ii), the dissipation rates decreased to approximately 5.9 mJ/mm^2.

4. Concluding remarks

In this work, the fracture behavior of Al/Zr and Zr/DU-10%Mo interfaces was measured via the miniature bulge test and the minicantilever bend techniques. The values for the Al/Zr fracture toughness, obtained from the miniature bulge test and the minicantilever beam bending, were in good agreement. However, the value of fracture toughness for the Zr/DU-10%Mo interface from minicantilever beam bending was higher than that obtained using the miniaturized bulge test.

This discrepancy can be attributed to the area of interfacial content measured by each test technique. That is, the miniature bulge test encompasses a larger amount of interfacial content, and so any inhomogeneity or weakness in the Zr/DU-10%Mo interface is more statistically likely to limit fracture toughness in this test method. However, the minicantilever test measures local fracture behavior at reduced interfacial areas. As such, the miniature bulge test represents a lower bound fracture toughness associated with inhomogeneities at the interface, whereas the minicantilever test represents an upper-bound fracture toughness value of a "pristine" interface.

5. Acknowledgements

The authors would like to acknowledge the financial support of the US Department of Energy Global Threat Reduction Initiative Reactor Convert program. Los Alamos National Laboratory, an affirmative action equal opportunity employer, is operated by Los Alamos National Security, LLC, for the National Nuclear Security Administration of the U.S. Department of Energy under contract DE-AC52-06NA25396.

6. References

[1] C. Liu, K.D. Clarke, K.J. Hollis, M.L. Lovato, D.J. Alexander, W.R. Blumenthal, and D.E. Dombrowski, "Measuring Fracture Toughness in LEU Fuel Plates Containing Al/Zr/DU-10wt%Mo Interfaces Using Miniature Bulge Test & 3D-DIC," Los Alamos National Laboratory Report, LA-UR-14-24547, 2014.

[2] W.M. Mook, J.K. Baldwin, R. Martinez, and N.A. Mara, "SEM *in situ* MiniCantilever Beam Bending of U-10Mo/Zr/Al Fuel Elements," Los Alamos National Laboratory Report, LA-UR-14-24435, 2014.

[3] J.D.G. Sumpter. *Fracture toughness - a measurable materials parameter*. in *FRACTURE, PLASTIC FLOW AND STRUCTURAL INTEGRITY*. 1 Carlton House Terrace, London SW1Y 5DB, England: Iom Communications Ltd.